

ornl

**OAK RIDGE
NATIONAL
LABORATORY**

MARTIN MARIETTA

A Hot-Cell Titration System

L. N. Klatt



OAK RIDGE NATIONAL LABORATORY
CENTRAL RESEARCH LIBRARY
CIRCULATION SECTION
1000 FT. BLDG. 213
LIBRARY LOAN COPY
DO NOT TRANSFER TO ANOTHER PERSON
If you wish someone else to see this
report, send in same with report and
the library will arrange a loan.

OPERATED BY
MARTIN MARIETTA ENERGY SYSTEMS, INC.
FOR THE UNITED STATES
DEPARTMENT OF ENERGY

Printed in the United States of America. Available from
National Technical Information Service
U.S. Department of Commerce
5285 Port Royal Road, Springfield, Virginia 22161
NTIS price codes—Printed Copy: A03 Microfiche A01

This report was prepared as an account of work sponsored by an agency of the United States Government. Neither the United States Government nor any agency thereof, nor any of their employees, makes any warranty, express or implied, or assumes any legal liability or responsibility for the accuracy, completeness, or usefulness of any information, apparatus, product, or process disclosed, or represents that its use would not infringe privately owned rights. Reference herein to any specific commercial product, process, or service by trade name, trademark, manufacturer, or otherwise, does not necessarily constitute or imply its endorsement, recommendation, or favoring by the United States Government or any agency thereof. The views and opinions of authors expressed herein do not necessarily state or reflect those of the United States Government or any agency thereof.

ORNL/TM-10780
Dist. Category UC-526

Consolidated Fuel Reprocessing Program

A HOT-CELL TITRATION SYSTEM

L. N. Klatt
Analytical Chemistry Division

Date Published – July 1988

NOTICE This document contains information of a preliminary nature.
It is subject to revision or correction and therefore does not represent a
final report.

Prepared for the
Office of Facilities, Fuel Cycle,
and Test Programs

Prepared by the
OAK RIDGE NATIONAL LABORATORY
Oak Ridge, Tennessee 37831
operated by
MARTIN MARIETTA ENERGY SYSTEMS, INC.
for the
U.S. DEPARTMENT OF ENERGY
under contract DE-AC05-84OR21400



3 4456 0281204 4

CONTENTS

ABSTRACT.....	v
1. INTRODUCTION.....	1
2. SYSTEM DESCRIPTION.....	3
2.1 Titrant Delivery Unit.....	3
2.2 Electronic System.....	6
2.3 Microcomputer Hardware.....	7
2.4 Software.....	7
3. PERFORMANCE OF THE SYSTEM.....	15
3.1 Potentiometric Titration System.....	17
3.2 Amperometric Titration System.....	24
REFERENCES.....	29

ABSTRACT

Operation of a nuclear fuel reprocessing plant requires an analytical support laboratory capable of meeting the process control, product quality, and nuclear safeguard requirements. Because of the radioactivity accompanying many of the samples, the analytical instruments must be selected, modified, or specifically developed for use in hot cells. Titrimetric procedures have been successfully used in hot cells and are generally immune to radiation induced bias. This report describes a titration system designed for operation in a hot-cell environment. The potentiometric titration system has operated successfully for four years in support of nuclear fuel reprocessing research and development activities. Details of the hardware, electronic, and software control and data analysis systems are presented. Interchangeable burets with a capacity of 5, 10, and 25 mL are available; the means of the absolute error in delivered volume for these burets are 0.9, 1.1, and 1.8 μL , respectively. Results of evaluation studies show that the accuracy and precision of analysis results obtained with the potentiometric system are limited by statistical uncertainties associated with the standard titrant, sample preparation procedure, and the equilibrium constant of the titration reaction and not by titrator performance factors. The system is also capable of performing amperometric titrations. Changing between the potentiometric and amperometric modes of operation involves changing the in-cell transducers, the in-cell electronics, and the titrator control program.

1. INTRODUCTION

The successful operation of a nuclear fuel reprocessing plant requires an analytical support laboratory capable of meeting, in a timely and cost-effective manner, the process control, product quality, and special nuclear safeguard analysis requirements. Because of the radioactivity accompanying the majority of the samples processed by this laboratory, the analytical procedures and instruments must be selected, modified, or specifically developed for use in remote environments such as glove boxes and hot cells.

Titration are among the most common laboratory procedures. It is estimated that two-thirds of the analytical requirements of a prototypical nuclear fuel reprocessing plant can be met by potentiometric titrations. Titrimetric procedures have been successfully used in hot cells and are generally immune to radiation induced bias. The primary advantage of titrimetric procedures is that the analytical result can be obtained from measurements of relative concentrations, thereby eliminating transducer calibration errors and minimizing errors associated with a variable or unknown sample matrix. The principal disadvantage of this methodology is that it is generally time and manpower intensive.

Automatic titrators usually employ one of three methods to determine the end point of a titration. The simplest automatic titrator adds the titrant until the transducer output attains some predetermined value and the end point is read directly from the buret. This type of automatic titrator is easy to operate and can perform the titration rapidly. However, it requires prior knowledge of the transducer output at the end point; consequently, errors due to transducer calibration and sample matrix are significant. The second type of automatic titrator adds the titrant at a constant rate, and a recorder plots the transducer output. The end point is obtained from this plot after the titration is completed. This approach is limited to systems with short transducer time constants and rapid reaction rates. The third type of automatic titrator adds the titrant in such a manner that the transducer output represents equilibrium or near equilibrium conditions. Successful implementation of this type of automatic titrator requires anticipating the end point.

Development of mechanical and electronic systems to automatically anticipate and measure the end point has been evolving for about 40 years. Lingane¹ described a potentiometric titration system that titrated to a predefined end point potential. It incorporated an anticipation system based upon the overshoot of the indicator electrode potential caused by placing the titrant delivery tube in proximity to the indicator electrode and the finite time required to mix the solution. Malmstadt and Felt² described the first application of an electronic differentiation circuit to automatically locate the end point. Because the differentiation was performed with respect to time, the titrant had to be added at a constant rate. End point bias resulting from mixing delays, electrode response time constants, and chemical reaction rates was minimized by standardization. Kelley, Fisher, and Wagner³ described the first system that performed the differentiation with respect to titrant volume and simultaneously used the magnitude of the derivative to control the rate of titrant addition. This system used a synchro generator and two synchro receivers to

provide a linear relationship between the volume of titrant delivered and the recorder chart drive. The derivative was approximated by the instantaneous error signal from the recorder servo system and was used to control the velocity of the synchro generator. The end point was manually located from the recorder plot. This system was the most advanced totally analog automatic titrator developed.

With the advent of inexpensive, integrated digital logic circuits and the laboratory minicomputer, numerous automatic titrators were developed,⁴⁻¹⁰ and considerable attention was given to the development of algorithms for automatic location of the end point and to the development of volume predictor algorithms,¹¹⁻¹⁴ (i.e., the digital analog to the anticipator circuits). Hunter, Sinnamon, and Hieftje¹⁵ described a totally digital automatic titrator. Titrant was added by a droplet generator, and digital filtering algorithms were employed to calculate the second derivative of the titration curve and to locate the end point. Christiansen, Busch, and Krogh¹⁶ described an empirical equation relating the volume increment to the slope of the titration curve which served as the volume predictor algorithm in a microcomputer controlled titrator. The end point was calculated by the microcomputer from the zero crossing point of the second derivative. Leggett¹⁷ described a microcomputer controlled titrator which used a volume predictor algorithm involving the instantaneous slope of the titration curve and a constant change in signal to calculate each volume increment. Smit and Smit¹⁸ discussed automatic titrators from a systems theory viewpoint.

This report describes a titration system specifically designed for operation in a hot-cell environment. A microcomputer controls the entire operation of the system. Four years of successful hot-cell operation as a potentiometric titrator have been achieved in support of nuclear fuel reprocessing research and development activities. By changing the in-cell transducers, signal conditioning circuit, and loading a different control program into the memory of the microcomputer, the system can perform amperometric titrations.

2. SYSTEM DESCRIPTION

The general arrangement of the remote titrator system is shown schematically in Fig. 2.1. The major system components are the in-cell titrant delivery unit, electronic systems (in-cell systems and computer interfaces), the microcomputer, and the software. Detailed features of the individual units are described below.

2.1 TITRANT DELIVERY UNIT

A prototype of the in-cell titrant delivery unit is shown in Fig. 2.2. It consists of four submodules: the delivery drive unit, the buret, the elevator, and the signal distribution box. The modular design was selected to facilitate remote maintenance of the system. The metal components are constructed from aluminum and stainless steel; the aluminum parts are anodized to produce a hard and durable surface. All nonmetal parts are fabricated from Teflon.

The operating principle of the titrant delivery unit is the piston displacement of liquid. The delivery drive unit consists of a 1.8° per step stepping motor (Model M062, Superior Electric Company, Bristol, Connecticut having a 0.46 N·m (65 oz.in.) torque driving a precision ground $1/4 \times 20$ lead screw. Attached to the motion conversion nut is a permanent magnet which actuates Hall effect proximity switches (Model 103SR12A-1, Micro Switch Inc., Freeport, Illinois) to stop the stepping motor at the full and empty positions of the buret. The end of the piston push rod connects to the buret piston with the coupling system shown in Fig. 2.3. The orientation of the piston push rod is fixed while the buret piston is free to rotate. When the piston push rod is positioned at the buret change position, this coupling system allows the buret to be removed and attached by merely sliding it horizontally.

The burets are designed to be interchangeable; capacities of 5, 10, and 25 mL can be accommodated. A three-way solenoid valve (Series-1-115-S, General Valve Corporation, Fairfield, New Jersey) mounted on the buret housing is used to control the direction of fluid flow during all movements of the buret piston. The buret is positioned on the delivery unit housing by a spring-loaded locating pin with a hemispherical end; it is securely clamped to the delivery unit housing by four wing nuts. The buret barrel is fabricated from precision bore Pyrex glass tubing (Wilmad Glass Co., Inc., Buena, New Jersey). Fluid seals are made with a neoprene rubber O-ring at the top of the glass barrel and a neoprene rubber O-ring mounted in the Teflon liner attached to the stainless steel piston. Tubing connections to the buret and solenoid are made with male Luer connectors screwed into the respective ports.

The elevator module is used to position the titration vessel under the electrodes and titrant delivery tube. It is powered by a reversible ac motor (Model TS25, Superior Electric Co., Bristol, Connecticut). Limit of travel signals are generated by Hall effect proximity sensors, which are actuated by a permanent magnet attached to the rear of the elevator table.

The signal distribution box connects to three multiconductor cables providing electrical circuits between the titrant delivery unit and the controller system located in the operator area of the hot-cell laboratory.

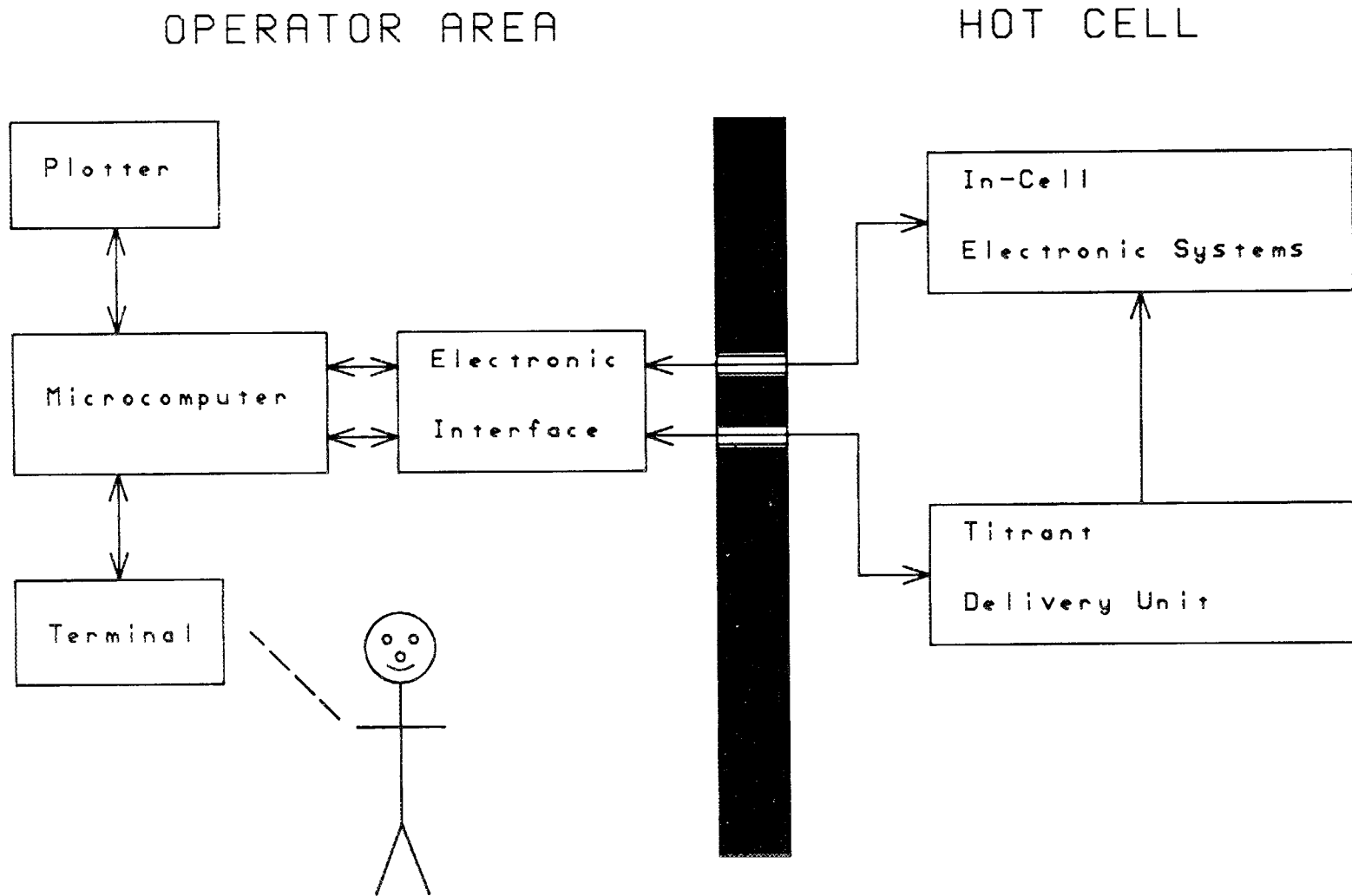


Fig. 2.1. Block diagram of remote titration system.

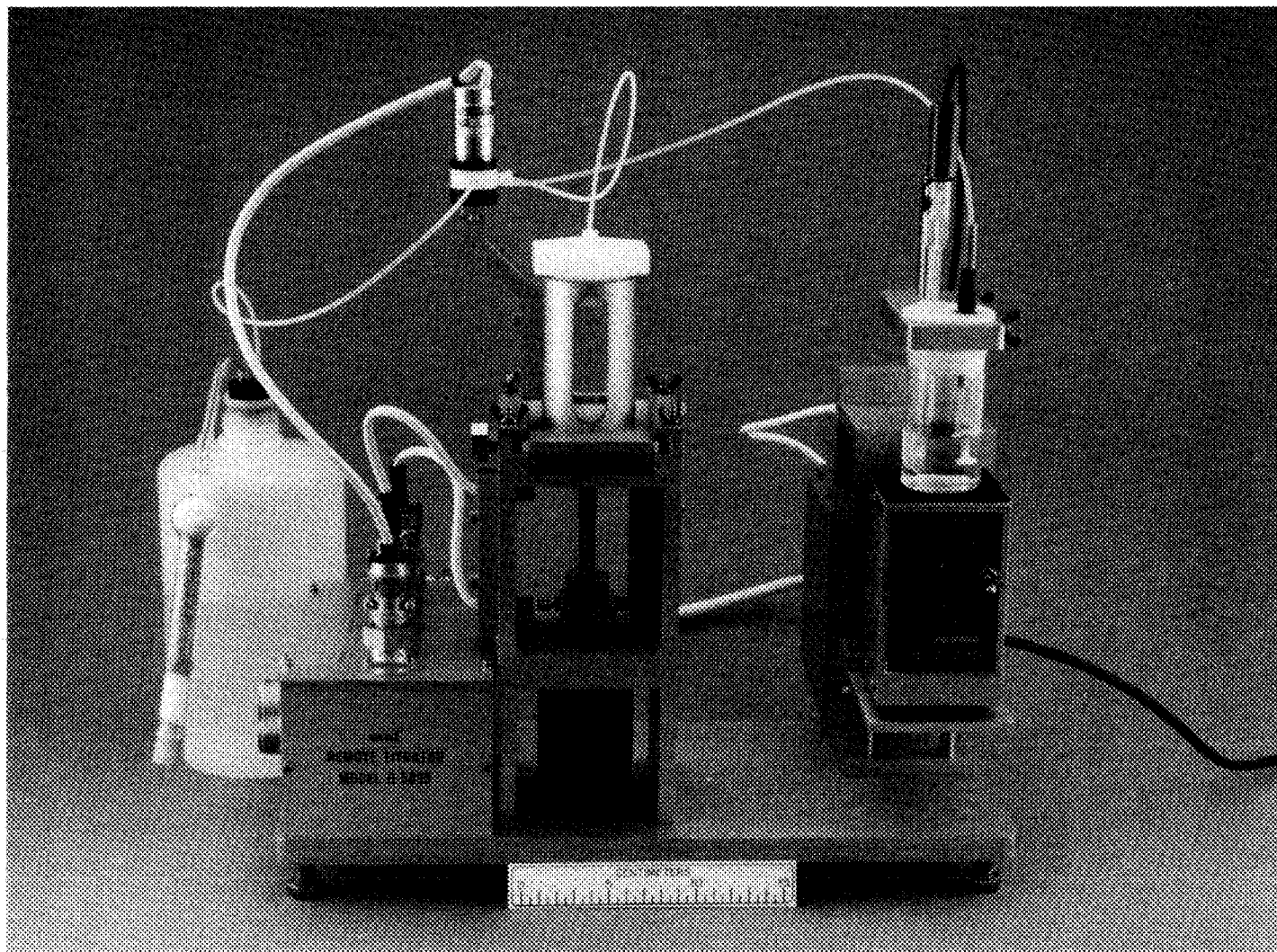


Fig. 2.2. Photograph of in-cell system of remote titrator.

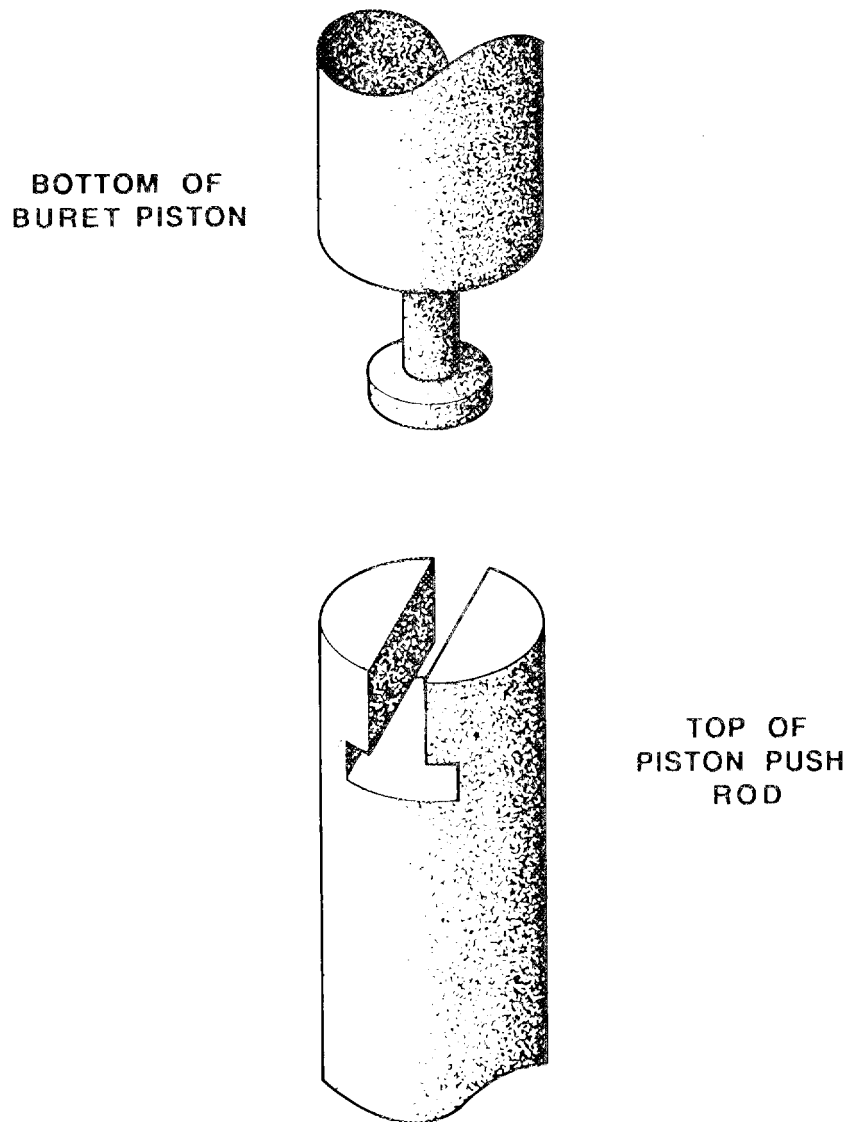


Fig. 2.3. Coupling system between the buret piston and the push rod.

2.2 ELECTRONIC SYSTEM

The electronic system consists of several submodules. Because of the number of signals required to operate the in-cell portion of the system and the type of cables available in the Transuranium Processing Plant at the Oak Ridge National Laboratory, a portion of the electronic system had to be located in the hot cell. These units are the transducer signal processing circuit

and the elevator control circuit. These circuits are contained on printed circuit boards and are housed in separate enclosures. They have been designed to allow replacement with the master/slave manipulators. The circuit boards can be inserted only when in the proper orientation.

The transducer enclosure is attached to the rear of the delivery unit housing (not shown in Fig. 2.2). Power and control signals from the microcomputer and the analog input signal to the microcomputer are provided by a multiconductor cable. Two different transducer signal processing circuits have been developed; one is a high input impedance amplifier required for potentiometric titrations, and the other is a potentiostat required for amperometric titrations. These circuits are shown in Figs. 2.4 and 2.5, respectively. The circuit shown in Fig. 2.4 illustrates the methods used to protect the in-cell amplifier inputs from large noise transients and accidental reversal of the polarity of the power supply connections. Each circuit is housed in a different enclosure, and to change the type of end point detection system requires disconnecting the signal cable from one enclosure and connecting it to the other enclosure.

The elevator control circuit is housed in an enclosure attached to the rear of the elevator assembly. The circuit diagram is shown in Fig. 2.6. The circuit is designed to allow only motion of the elevator platform between upper and lower limits. The operator activates this circuit by means of switch SWI, which is located in the operator area of the hot-cell laboratory.

The stepping motor is driven by a translator module (Model STM-103, Superior Electric Company). Digital inputs are available for determining the direction of motor rotation and for gating an on-board variable frequency oscillator, which determines the motor stepping rate. These digital inputs are controlled by the custom interface board installed in the computer chassis. The translator module, stepping motor power supply, and the elevator and stirrer motor controls are mounted in a chassis, which is located within convenient reach of the hot-cell operating face.

2.3 MICROCOMPUTER HARDWARE

The controller for the titrator is a microNOVA MP/100 microcomputer (Data General Corporation, Westboro, Massachusetts). The 16-bit system processing unit with an integral asynchronous serial communication port is located on a single board. The memory for the system consists of 8,192 words of random access memory (RAM) and 24,576 words of electrically programmable read-only-memory (EPROM). An additional asynchronous serial communication board is used to communicate with the digital plotter. A digital input/output board is used to interface the microcomputer with the custom interface card, which contains the analog-to-digital converter, stepping motor control logic, and relay driver circuitry. This custom interface board has been described.¹⁹ When the titrator is configured for amperometric titrations, a digital-to-analog converter is required to set the potential at which the amperometric titration is being performed. The microcomputer power supply and the above boards are housed in the MP/100 chassis. Operator interaction with the system is from a rack mounted terminal.

2.4 SOFTWARE

Software for the titrator is written in FORTRAN. Assembly language subroutines for the analog-to-digital converter, digital-to-analog converter, stepping motor, relay driver, buret limit signals, and a memory test routine are included. The FORTRAN and assembly language modules are linked to a stand-alone subset of the operating system. The resulting executable code is programmed into EPROM chips, which upon installation in the MP/100 memory boards results in a stand-alone control system for the titrator. The complete program occupies about 22,000 words of EPROM memory.

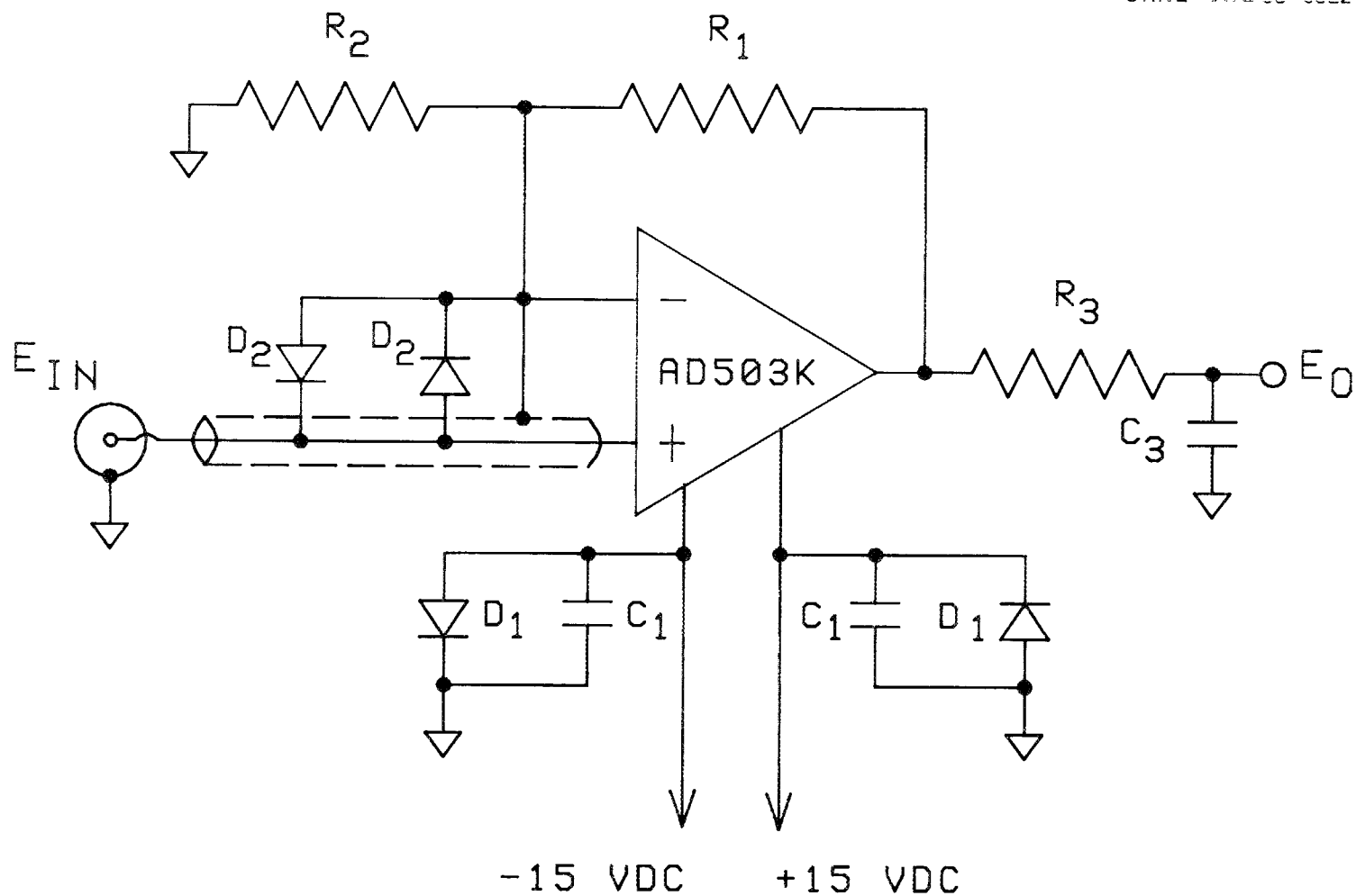


Fig. 2.4. Partial schematic diagram of the in-cell transducer preamplifier for the potentiometric titrator:
 $R_1 = 4\text{K} \pm 0.5\%$, $R_2 = 1\text{K} \pm 0.5\%$, $R_3 = 2\text{K}$, $D_1 = 1\text{N4004}$, $D_2 = 1\text{N459A}$, $C_1 = 0.01\ \mu\text{F}$, and $C_3 = 1.0\ \mu\text{F}$.

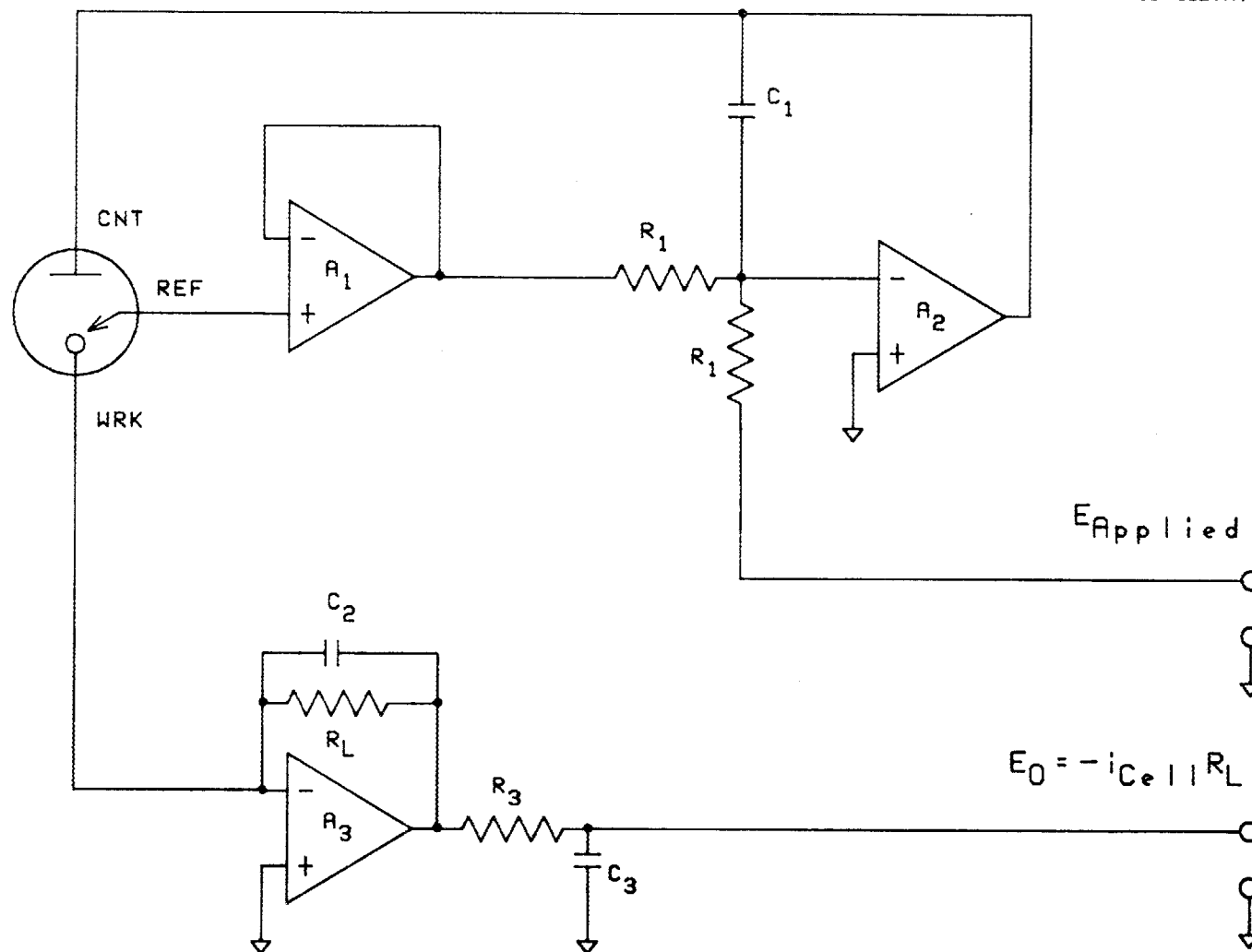


Fig. 2.5. Partial schematic diagram of the in-cell transducer control circuit for the amperometric titrator: $A_1 = \text{LM310H}$, $A_2 = \text{MC1741SC}$, $A_3 = \text{AD503K}$, $R_1 = 5 \text{ K}$, $R_L = 40 \text{ K}$, $R_3 = 3.9 \text{ K}$, $C_1 = 0.33 \mu\text{F}$, $C_2 = 0.01 \mu\text{F}$, and $C_3 = 4.4 \mu\text{F}$.

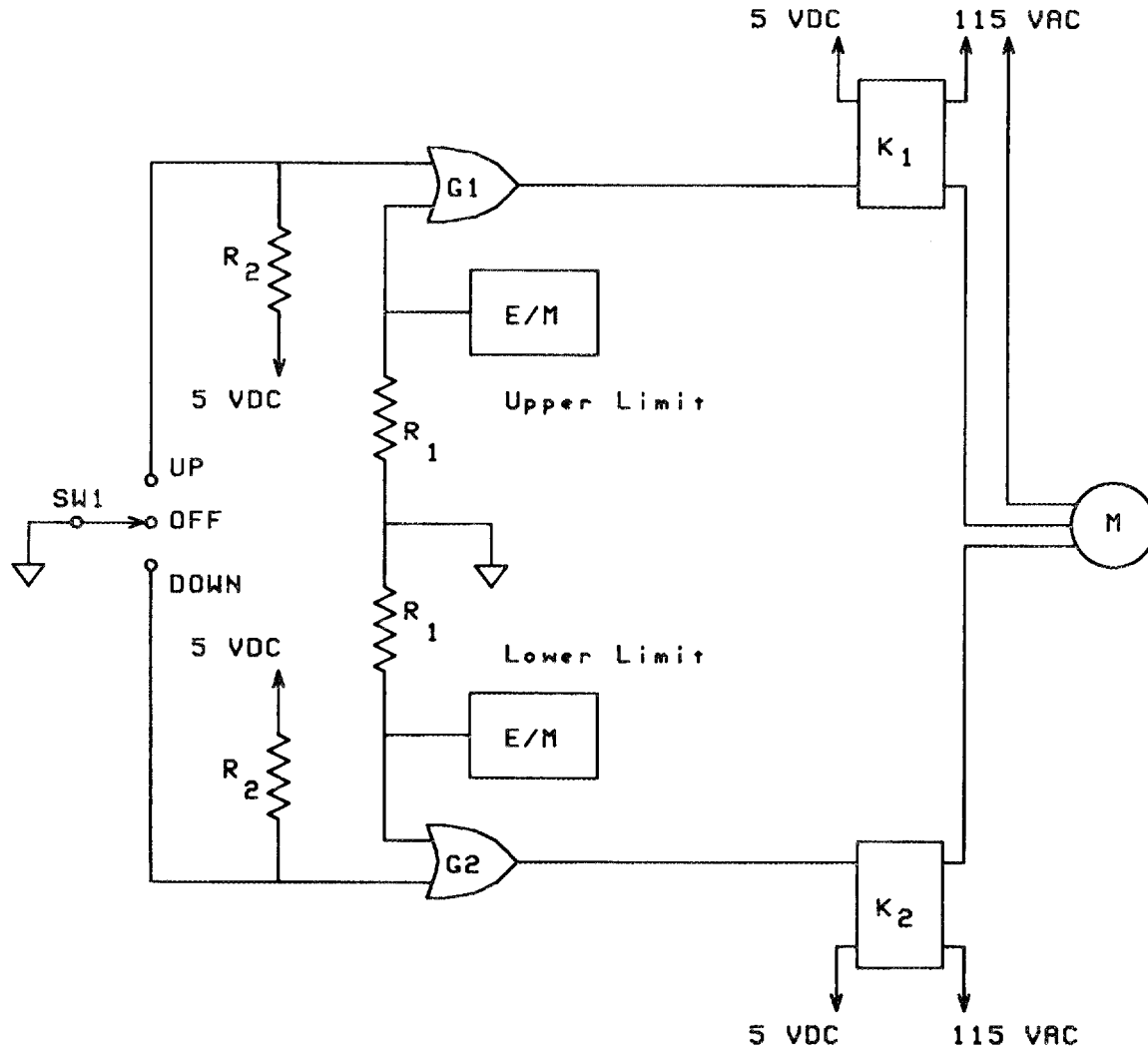


Fig. 2.6. Partial schematic diagram of the elevator control circuit: $R_1 = 240$, $R_2 = 2.2 \text{ K}$, $G_1 = G_2 = 1/4$ of SN7432, and $K_1 = K_2 =$ Teledyne 641-1.

The software is written as a multitasking program. This allows operator intervention at critical points during execution of selected functions. For example, when a titration is initiated two separate tasks are started. The first task consists of all the operations required to perform the titration, such as data acquisition, data analysis, plotting of the data, and reporting status information on the terminal display. The second task monitors activity on the terminal keyboard. Entry of any information causes an orderly termination of the titration task. The benefit of this multitasking approach is that execution of options can be terminated at any time by the operator without the need to invoke any commands or termination protocol, and if desired, it can be reinitiated with all task parameters intact or with a new set of parameters.

The approach taken throughout the control program is to present to the operator a menu of currently available options and the necessary system status. Operator control of the system occurs through the main menu, from which he instructs the system to execute any of the functions listed in Table 2.1. The number represents the code the operator enters to select the function. After selection of an option the system displays it and then requires the operator to verify the selection. A detailed description of each function is contained in the operating manual.²⁰

**Table 2.1. Options from main menu
of titrator control program**

0 = OPTIONS
1 = SERVICE
2 = PRIME
3 = EMPTY
4 = FILL
5 = TITRATE
6 = END POINT
7 = DELIVER
8 = REPLOT
9 = NEW BURET

The software was written to be totally tolerant of operator errors. This was accomplished by coding the program so that all input from the terminal occurs as a string variable. This results in every key on the keyboard being a valid input at all times. The program checks this information to ascertain whether valid data, within the context of the program, has been received.

Table 2.2 contains a section of the FORTRAN coding which illustrates the error checking and how the system responds to operator error. Statement 800 provides the prompt to the operator for the desired input. The Z at the end of FORMAT statement suppresses the line feed and carriage return normally appended to the output record so that the operator's response appears on the same line as the prompt. In this example, the program is requesting numeric information. The statement CALL INPUT performs the input as a string and decodes it to generate the numeric value stored as variable ADOS. The variable IER is an error code which denotes whether the decoding of the string was successful or, if not, what type of error prevented the decoding. When a value other than zero is returned, the program reports the error message and then requests the operator to reenter the information. If the error code is zero, the program then checks to ensure that the numeric value is within the allowed range of values for that variable. If not, the system reports that the value entered was invalid and requests the operator to reenter the information. It is important to note that the program does not exit from an input segment until valid datum is obtained.

Table 2.2. Program segment illustrating error handling

```

C
C   INPUT PREDOSE VOLUME IN MILLILITERS
C
800  WRITE(10,810)
810  FORMAT(" PREDOSE VOLUME IN ML: ",Z)
C
C   ENTER DATA AS A STRING ARRAY AND DECODE TO OBTAIN
C   THE NUMERIC INFORMATION VIA SUBROUTINE INPUT
C
      CALL INPUT(ADOS,IER)
      IF(IER .EQ. 0)GO TO 815
      WRITE(10,260)IER
260  FORMAT("INPUT ERROR ",12)
      GO TO 800
815  PREDOSVOL = INT(1000.0*ADOS)
      IF(PREDOSVOL .LT. VOLMIN .OR. PREDOSVOL .GT.
1INT(BURSIZE)GO TO 820
      RETURN
820  WRITE(10,830)
830  FORMAT(" INVALID PREDOSE VOLUME")
      GO TO 800

```

The control strategy for execution of a titration depends upon the type of titration (i.e., potentiometric or linear). For potentiometric titrations, the recording of equilibrium data in the end point region of the curve is important, while for a linear titration (e.g., an amperometric titration), the recording of equilibrium data in the pre-end point and post-end point regions of the curve are important.

In potentiometric titrations, the size of the volume increment added and the time required to achieve equilibrium after the addition are important parameters. Algorithms to control both of these are included in the software.

The volume increment algorithm is defined by Eq. (2.1),

$$V_{NEW} = 1000 \cdot \Delta / \text{SLOPE} \quad (2.1)$$

V_{NEW} is the predicted volume increment, Δ is the magnitude of the signal change desired upon addition of the volume increment, and SLOPE is the current slope of the titration curve. The magnitude of Δ is fixed at 3 mV. The sign of Δ must always equal the sign of SLOPE to accommodate different types of potentiometric titrations as well as provide numerical stability in the presence of noise. The slope is obtained from a two-term Taylor series, which is fit to the five most recent potential and volume data points via a least squares criterion. To allow the Taylor series to follow the curvature in the titration curve, the volume axis is translated about the midpoint of the five volume points used for the curve fitting. Evaluating the slope of the titration

curve from a Taylor series also minimizes the possibility of attempting to perform a division by zero in Eq. (2.1). If the calculated value of VNEW is larger than a specified maximum volume increment, the maximum volume increment is added, and if less than a specified minimum volume increment, the minimum volume increment is added. These maximum and minimum volume increments are determined by the size of the buret installed on the system.

Each minimum volume increment is tagged to denote the possible entry into an end point region of the titration curve. When three successive minimum volume increments are added, the control program assumes that an end point region of the titration curve is being traversed, and the system continues to add the minimum volume until Eq. (2.1) fails to predict the minimum volume or until at least 16 minimum volume increments have been added.

The volume predicting algorithm embodied in Eq. (2.1) is not self-starting. The initial point plus four equal subdivisions of the predose volume are used to start the algorithm. It should be noted that the predose volume also serves to decrease the amount of time required to perform a titration by adding a significant portion of the titrant in rather large volume increments.

Equilibrium conditions are achieved by employing delays between the cessation of the addition of each increment of titrant and the reading of the transducer output. Two delay options are available. One delay option requires the operator to specify the delay time; this can range from 250 ms to 60 s. The other delay option is an automatic mode in which the computer continually reads the transducer output, and when the drift has decreased to 1 mV/s or 30 s has elapsed, the current transducer reading is taken as the equilibrium reading.

For linear titrations a constant volume increment is adequate;¹² this method has been incorporated into the system. The delay algorithms described for the potentiometric titrations are used in the linear titration system.

The algorithm for calculating the end point of a titration depends upon the type of titration. For the potentiometric system, locating the zero crossing point of the second derivative of the signal with respect to volume is the preferred method.^{15,18} Two different methods of calculating the end point are included in the potentiometric titration system; one is automatically implemented upon completion of the titration, and the other is a manual method requiring operator input. The manual end point option is provided to allow reevaluation of end points which are either misplaced by the automatic routine or which are missed altogether because the end point break is too small.

The automatic end point calculation routine uses a digital filter technique²¹ to calculate the second derivative of the titration curve using only those volume points corresponding to the addition of the minimum volume increment. The end point is obtained from the volume intercept of a straight line fitted between the maximum and minimum values of the second derivative versus volume data.

The manual end point option calculates the end point from the volume intercept of the second derivative of Eq. (2.2).

$$P(V) = a_0 + a_1V + a_2V^2 + a_3V^3 \quad (2.2)$$

The coefficients a_0 , a_1 , a_2 , and a_3 are obtained by fitting Eq. (2.2) to the titration data between two operator specified volume points using a least squares criterion. V is the volume which has been translated on the volume axis about the midpoint of the volume region being fitted in order to allow the model equation to handle the curvature of the end point region.

For an ideal, linear titration curve the second derivative should be zero before and after the end point and, depending upon the magnitude of the equilibrium constant for the titration reaction, exhibit behavior in the end point region similar to that observed when a step function is differentiated. Because of dilution effects and noise on the transducer signal, a nonzero second derivative is usually observed in both the pre-end and post-end point region of the curve.

The algorithm to automatically sense the end point region of the amperometric titration curve compares the instantaneous value of the second derivative to an operator specified threshold value and tags those volume points at which the second derivative exceeds the threshold as end point region data. The second derivative is obtained through use of a digital filter.²¹ Typically, seven additional volume increments are added to define the post-end point region of the titration curve.

Because linear titration techniques are usually applied to chemical systems with smaller equilibrium constants than potentiometric titrations, curvature is usually present in the end point region of the titration curve, and methods for calculating the end point volume must use data removed from this region. Common practice involves extrapolating to the end point region by calculating the intersection of two line segments that are fit to pre-end and post-end point data. This approach has been implemented in the amperometric titration system in the automatic and manual mode. In the automatic mode those data points tagged by the end point sensing algorithm are not included in either the pre-end point or post-end point line segments. The manual implementation of the end point calculation differs only in that the operator must input starting and ending volume values for each region of the titration curve. These values can include points tagged by the end point sensing algorithm in the pre-end point and post-end point line segments, but the two regions cannot overlap.

As shown in Table 2.1, the control program for the titration systems includes a service routine. Upon selection of this option one can read the input voltage of the analog-to-digital converter, operate the buret solenoid, obtain the status of the buret limit of travel signals, operate the stepping motor, test the digital plotter, or output an analog voltage from the digital-to-analog converter. Faults can be diagnosed through appropriate use of the options in this service routine system. The service option also allows the system to be used for special analytical measurements because access to each measurement and control feature is provided.

3. PERFORMANCE OF THE SYSTEM

The accuracy and precision of the volume delivery system of the titrator are important parameters in determining the ultimate accuracy and precision of any analysis performed by the system. Data for delivery of aliquots of water for 5-, 10-, and 25-mL capacity burets are summarized in Tables 3.1, 3.2, and 3.3, respectively. The volume of each aliquot was determined from the mass, temperature, and density of water. Buoyancy corrections were applied to the weight data. The standard deviation values include the contribution from the mass measurement, which is estimated to be 0.3 μL . For the 5-mL buret, the mean of the absolute value of the error is 0.9 μL , and the mean standard deviation is 0.8 μL . Cumulative volume delivery data were also obtained during the measurement of the data summarized in Table 3.1. The cumulative volume is the total volume delivered during acquisition of each data set; the nominal value was 10.6500 mL. The mean of the observed cumulative volume for five replicate measurements was 10.6512 mL with a standard deviation of 1.7 μL . It is important to note that several refillings of the buret were required to obtain these data. For the 10-mL buret, the mean of the absolute value of the error is 1.1 μL , and the mean standard deviation is 2.1 μL . For the 25-mL buret, the mean of the absolute value of the error is 1.8 μL , and the mean standard deviation is 1.8 μL . In terms of digital resolution, the results contained in Tables 3.1-3.3 correspond to a maximum uncertainty of ± 2 steps of the stepping motor. The individual and cumulative aliquot delivery data indicate that the titrant delivery unit performs its task with high accuracy and precision.

Table 3.1. Aliquot delivery data obtained with a 5-mL capacity buret^a

Nominal volume (μL)	Mean of delivered aliquot (μL)	Std dev (μL) ^b
50	49.4	0.6
100	100.0	0.4
300	300.3	0.6
700	700.4	0.6
1500	1500.4	1.8
3000	3002.4	0.7
5000	4998.0	0.6

^aMotion of one step by the stepping motor corresponds to 0.5 μL .

^bSix measurements were taken, except only five were taken at 100 μL .

Table 3.2. Aliquot delivery data obtained with a 10-mL capacity buret^a

Nominal volume (μL)	Mean of delivered aliquot (μL)	Std dev (μL^b)
50	49.3	1.3
100	99.2	1.9
300	299.9	2.4
700	699.8	3.7
1500	1500.6	1.3
3000	2998.0	3.1
5000	5000.4	4.2
7500	7500.0	0.9
10000	9995.1	0.3

^aMotion of one step by the stepping motor corresponds to 1.0 μL .

^bSix measurements were taken.

Table 3.3. Aliquot delivery data obtained with a 25-mL capacity buret^a

Nominal volume (μL)	Mean of delivered aliquot (μL)	Std dev (μL^b)
50	49.2	0.7
100	99.7	2.1
300	299.4	2.9
700	699.1	2.6
1000	999.2	0.2
3000	2999.6	1.4
7000	7002.1	3.6
12000	12007.2	0.4
20000	20003.4	2.1

^aMotion of one step by the stepping motor corresponds to 2.5 μL .

^bFive measurements were taken, except at 700 μL , 7 mL, 12 mL, and 20 mL, ten, six, four, and three measurements, respectively.

3.1 POTENTIOMETRIC TITRATION SYSTEM

Noise on the signal from the transducer can determine the accuracy and precision of the analytical results as well as have a significant influence upon the performance of the control system. The noise of the in-cell preamplifier was measured. A combination pH electrode (Corning No. 476056) was immersed in a stirred aliquot of standard pH buffer. At pH 4 and 10, the observed RMS noise was 0.14 mV referred to the amplifier input; drift was not statistically different from zero. Since the signal change specified for the volume predictor algorithm is 3 mV, the signal-to-noise ratio of the data used in the titration control algorithm is 21:1.

Numerous titrations were performed to evaluate the analysis capabilities of the total system. Precision as a function of equilibrium constant of the titration reaction, buret capacity, and the ability of the system to automatically handle multiple end points was examined. Table 3.4 summarizes the observed precision data. It should be noted that although the equilibrium constant for the U(IV)-Cr(VI) reaction is very large, the observed titration curve is similar to that observed for the titration of NaH_2PO_4 with a strong base. Samples were selected to approximate the type of behavior expected with real samples in a nuclear fuel reprocessing plant. Typical titration curves are shown in Figs. 3.1 and 3.2.

Several important conclusions can be drawn from the data in Table 3.4. First, the standard deviation of the end point volumes are larger than the corresponding volume delivery data. This indicates that in routine use of the instrument, factors other than volume errors will determine the precision of the analytical results. Second, although the data suggests that the precision improves with the 5-mL buret, there is insufficient information available to statistically defend the trend. Third, as predicted by theoretical descriptions of titration curves, the standard deviation increases dramatically when dealing with very small breaks [e.g., $\text{HNO}_3 + \text{Al}(\text{NO}_3)_3$, $\text{HCl} + \text{acetic acid}$, and boric acid]. It is significant to note that the titration curves obtained from these three samples are quite similar to those observed for samples from a nuclear fuel reprocessing plant requiring an excess acid measurement in the presence of hydrolyzable heavy metal ions.

Figures 3.1 and 3.2 demonstrate the self-documentation features of the titration system. The date and time information denotes when the titration was executed and is automatically obtained from the time and date routines of the operating system software. The remaining information is provided by the operator and completely documents each titration. The segment of the program requesting this information is written so that the operator only needs to edit this information to reflect changes for each sample being titrated. It should be noted that burets of different capacity were used to perform these titrations and that the system can handle multiple end points even when they are poorly defined. The location of the end point between two data points for the titration shown in Fig. 3.1 shows the extrapolation aspect of the automatic end point calculating algorithm.

Actual titration curves for the determination of excess acid in the presence of uranium and plutonium are shown in Figs. 3.3 and 3.4, respectively. The curve of Fig. 3.3 is the titration of a quality control sample for the measurement of excess acid in the presence of uranium. The first break corresponds to the excess acid, and the second end point corresponds to the amount of hydrolyzable metal ion. The titration medium is 10 M LiCl. The titration curve in Fig. 3.4 is for the determination of excess nitric acid in a sample from the reprocessing of spent reactor fuel. This sample contains uranium and plutonium. The titration medium is also 10 M LiCl.

The manual end point calculation option described in Sect. 2.4 is designed to provide a means of evaluating end points missed by the automatic algorithm. Its primary application is with

Table 3.4. Observed precision of typical potentiometric titrations

Sample	log K_{eq}	Mean end point		No. of replicates
		volume (mL)	Std dev (mL)	
HNO ₃ ^a	14.0	4.036	0.009	3
HNO ₃ + Al(NO ₃) ₃ ^a	14.0	4.030 ^b	0.085	4
HCl ^a	14.0	4.136	0.008	4
HCl ^c	14.0	12.536	0.006	8
HCl + acetic acid ^c	14.0	5.296 ^d	0.219	5
H ₃ PO ₄ ^a	11.8	2.197	0.001	4
H ₃ PO ₄ ^c	11.8	7.827	0.014	4
HCl + acetic acid ^c	9.2	17.175 ^e	0.017	5
Acetic acid ^a	9.2	2.473	0.005	4
Acetic acid ^c	9.2	12.161	0.010	4
Potassium phthalate ^c	8.6	14.744	0.005	4
NaH ₂ PO ₄ ^a	6.8	4.454	0.004	4
NaH ₂ PO ₄ ^c	6.8	15.670	0.012	4
H ₃ BO ₃ ^a	4.8	2.663 ^b	0.011	4
H ₃ BO ₃ ^c	4.8	11.355	0.193	3
U(IV) ^f	35.0	7.432 ^g	0.027	4

^a5-mL buret with 0.1000 M NaOH titrant.

^bRequired the execution of the manual end point algorithm.

^c25-mL buret with 0.2002 M NaOH titrant.

^dHCl end point is the first end point.

^eAcetic acid is the second end point. Value is the total titrant volume added to the second end point.

^f25-mL buret with 4.181 mM K²Cr²O₇. A platinum indicator and saturated calomel electrode pair served as the transducer.

^gSample was 1 mL of a 21.24-mg/mL solution.

very small end point breaks; however, it can also be used to reevaluate end points misplaced by the automatic algorithm. Data in Table 3.5 summarize the differences observed between the two end point calculating procedures. The standard deviation of the least squares fit is a measure of the goodness of fit. The results show that Eq. (2.2) indeed works best for the very small end point breaks. The uncertainty of the mean value for the HCl + acetic acid mixture indicates that Eq. (2.2) does not introduce any bias into the end point values. However, differences of $\pm 2\%$ should be expected for any given titration; the magnitude of these differences agree with the inherent precision of these titrations.

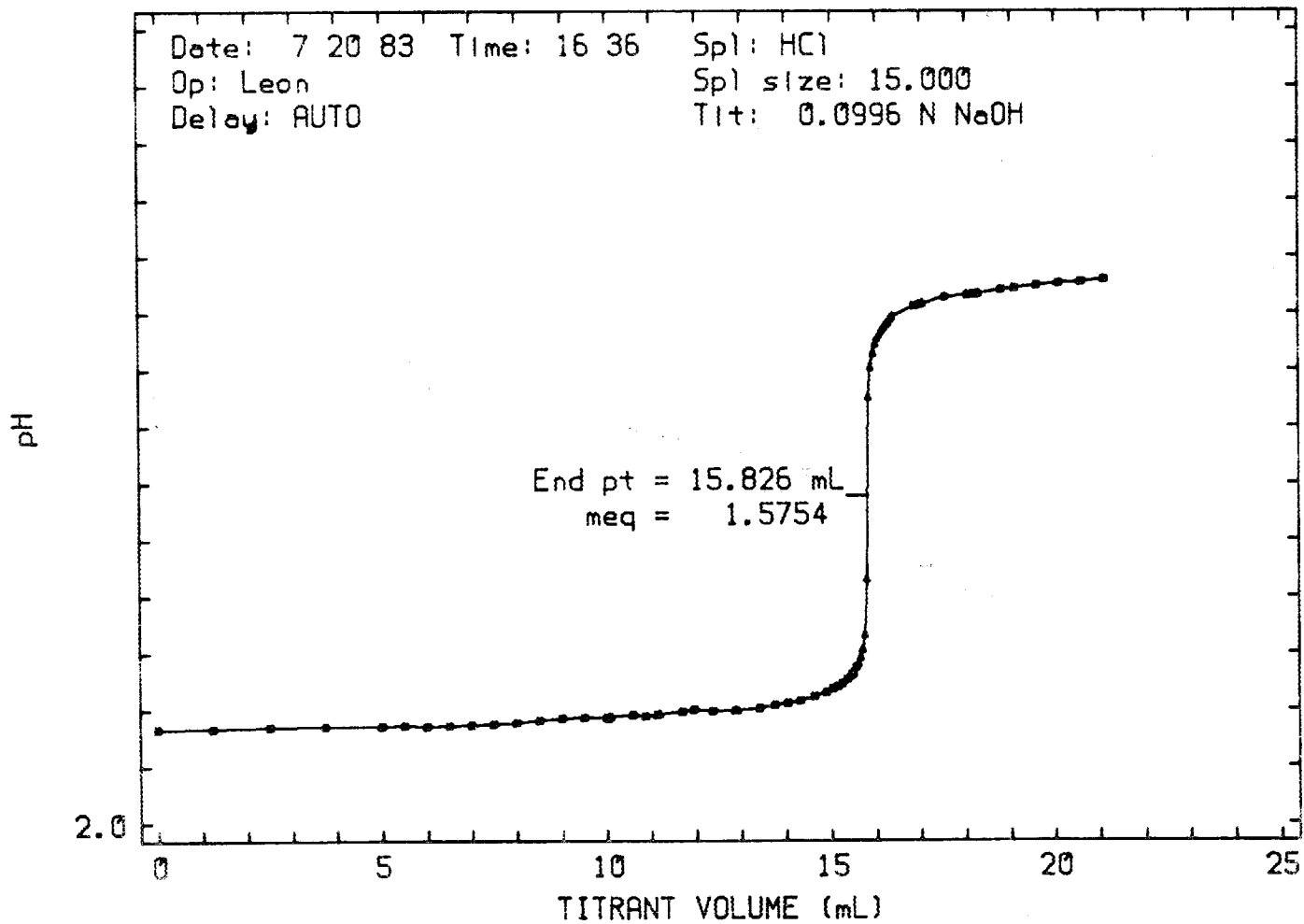


Fig. 3.1. Titration curve of a single end point system.

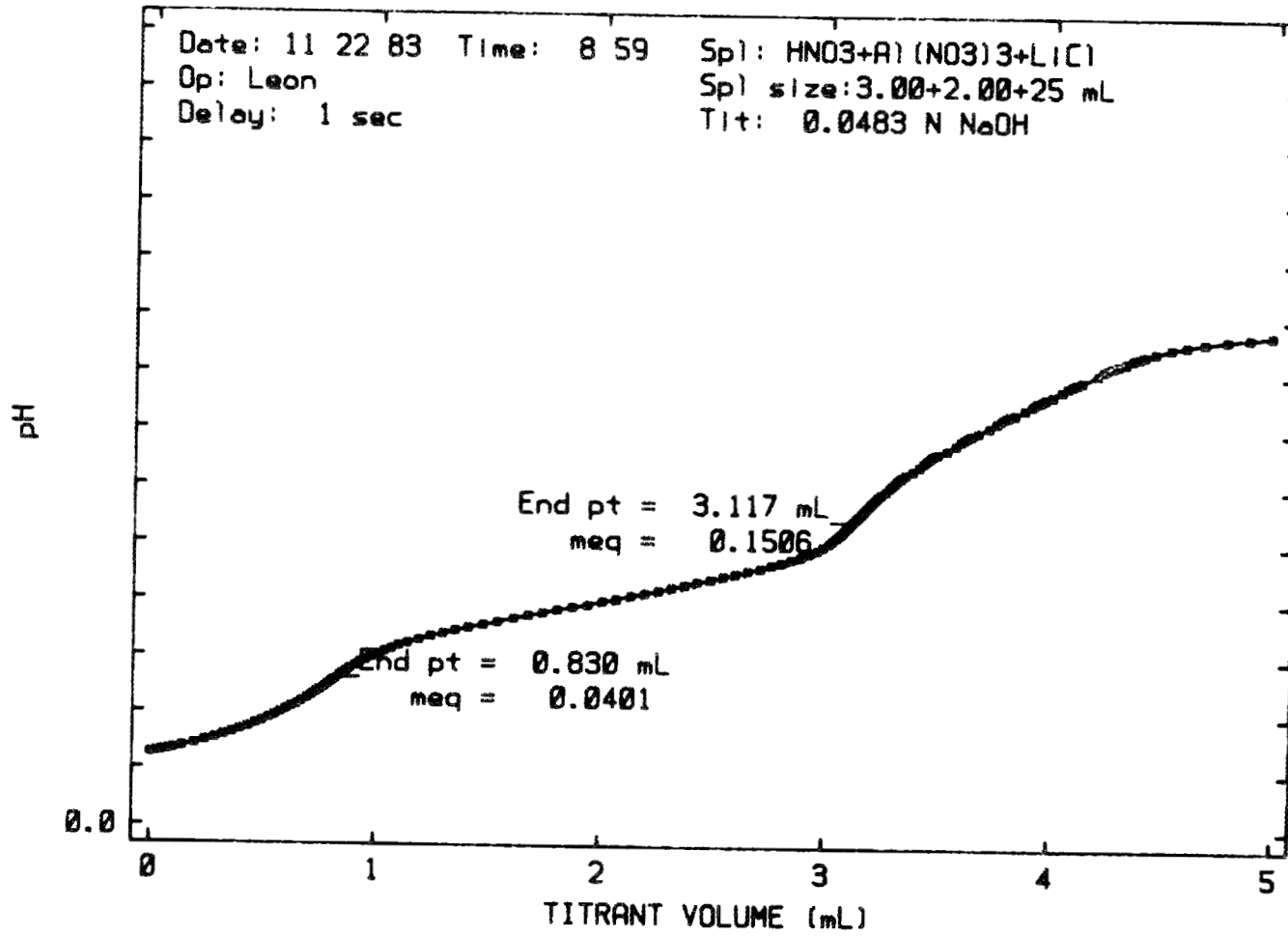


Fig. 3.2. Titration curve of a multiple end point system.

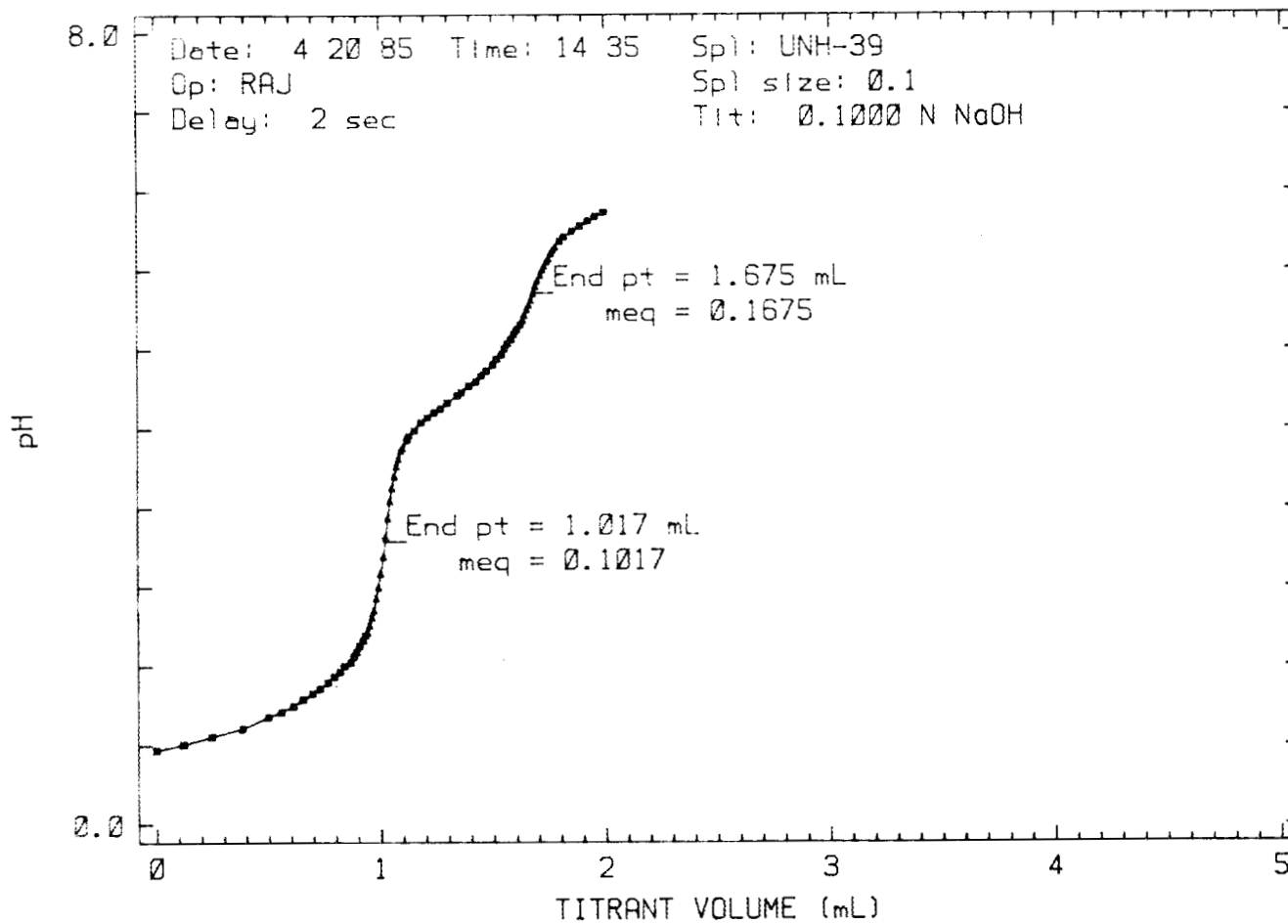


Fig. 3.3. Titration curve of a quality control standard for free acid and total hydrolyzable metal ion.

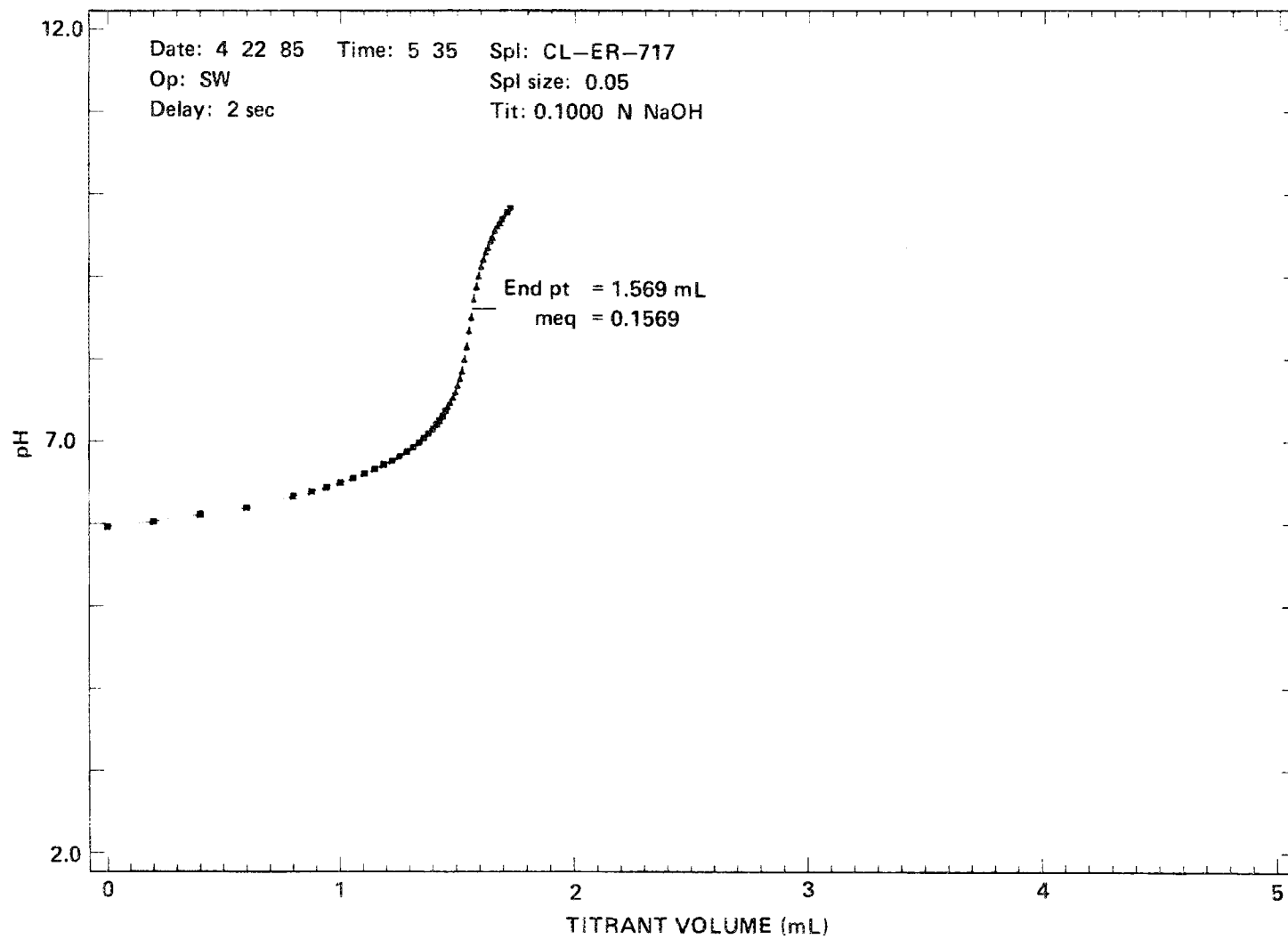


Fig. 3.4. Titration curve of a process solution submitted for measurement of free acid in the presence of hydrolyzable heavy metal ion.

Table 3.5. Comparison of the manual and automatic end point algorithms

Sample	% Difference	Std dev of least squares fit (mV)
H ₃ BO ₃	-1.4	0.5
HCl + acetic acid	0.6 ± 1.0 ^a	1.0
H ₃ PO ₄	1.9	8.6
NaH ₂ PO ₄	-0.8	9.5

^aResults are for the HCl end point from eight replicate titrations.

The accuracy of the analysis obtained with the system is not only influenced by the factors discussed above but also is influenced by the precision of the titrant standardization procedure. Data illustrating the precision of a typical standardization are shown in Table 3.6. The mean molarity is 0.09955 with a standard deviation of 0.00010. The estimated standard deviation in the weight of potassium phthalate is 0.0003 g. Assuming that the total variance of the mean molarity is composed of contributions from the mass of standard reagent, the end point determination, and the volume delivery and that the relative variances are additive, the estimated standard deviation of the end point determination is 0.013 mL. Clearly, the precision and accuracy of analytical results obtained with the remote titration system are, except in very special circumstances, determined by the sample treatment procedures and the underlying thermodynamics of the titration reaction and not by instrument performance.

Table 3.6. Typical data for the standardization of NaOH titrant

Grams of potassium phthalate	Molarity of NaOH
0.4010	0.09949
0.3992	0.09947
0.3910	0.09963
0.4404	0.09942
0.3798	0.09964
0.4037	0.09966

3.2 AMPEROMETRIC TITRATION SYSTEM

To perform an amperometric titration, a known voltage is applied to an electrochemical cell, and the resulting current flow is measured as a function of the volume of titrant added. An important element in this titration system is the electronic circuit used to control the cell potential and measure the current. The circuit shown in Fig. 2.5 employs a negative feedback control system, amplifier A_2 , to maintain the cell potential E_{WRK} versus E_{REF} equal to the applied potential, E_{Applied} . Amplifier A_1 provides the necessary impedance matching between the electrochemical cell and the low impedance load that R_1 provides to the summing point of A_2 . Amplifier A_3 is a current-to-voltage converter (i-E) and maintains the indicator electrode potential at circuit common voltage. Use of an i-E converter to measure the current eliminates need for a positive feedback circuit to correct for any $i_{\text{cell}}R_L$ losses. The low-pass filter, R_3C_3 , limits the bandwidth of the signal sampled by the computer.

Key factors in the use of this control circuit are the accuracy of the control function and the stability of the circuit as a function of frequency when connected to the electrochemical cell. Figure 3.5 shows the transfer function of the electrochemical cell driven by the control circuit depicted in Fig. 2.5. These data were obtained with an electrochemical cell composed of a saturated calomel reference electrode, SCE, (Corning No. 476002) and platinum counter electrode and indicator electrodes (Corning No. 476060). These electrodes were positioned symmetrically on a circle of 9.5-mm (0.375 in.) radius. The electrolyte was 1 M H_2SO_4 . The left ordinate axis corresponds to the magnitude of the ratio of $e_{\text{REF}}/e_{\text{Applied}}$, and the right ordinate axis corresponds to the phase angle of e_{REF} with respect to e_{Applied} ; these values should be 1.0 and -180° for accurate control. Since amperometric titrations are performed essentially at zero frequency, the circuit has adequate control accuracy. The roll off with increasing frequency is determined by C_1 . The shape of the curves in Fig. 3.5 indicates that the circuit is unconditionally stable.

Since the amperometric system will be used primarily for the analysis of plutonium, the evaluation of the system was restricted to this single application. The standardization portion of the procedure for the analysis of nuclear grade plutonium dioxide²² was used. Fe(II) is the titrant in both the standardization and Pu measurement steps. $\text{K}_2\text{Cr}_2\text{O}_7$ is used as the oxidant to standardize the Fe(II) solution. A typical titration curve is shown in Fig. 3.6. The plus sign marks the end point, and the radius of the circle indicates the estimated uncertainty of the end point.

The results of the evaluation are summarized in Fig. 3.7. The ordinate is the ratio of the measured end point volume to the aliquot volume. The regression equation for the data contained in Fig. 3.7 is

$$V_{\text{end point}}/V_{\text{aliquot}} = 0.5411 \pm 0.0010 + (3.8 \pm 18.5 \times 10^{-5})V_{\text{aliquot}} \quad (3.1)$$

The two curves shown on the plot correspond to the 95% confidence interval about this regression equation. The magnitude of the uncertainty in the slope term of Eq. (3.1) confirms that the results are independent of the sample size. The uncertainty of the intercept indicates that the relative precision observed during this study was 0.2%. The noise on the measured current is <50 nA ($R_L = 40$ k Ω) in the pre-end point region and appears to be directly related to the magnitude of the current in the post-end point region. The aliquots of $\text{K}_2\text{Cr}_2\text{O}_7$ ranged from 0.02702 to 0.2161 meq, which in terms of the mass of ^{239}Pu required for an analysis corresponds to a sample range from about 3.2 to 26 mg. It is important to note that in this study sample aliquots were prepared with standard glass transfer pipets, and these were not calibrated one relative to another. Normally, weight burets are used when plutonium samples are analyzed.

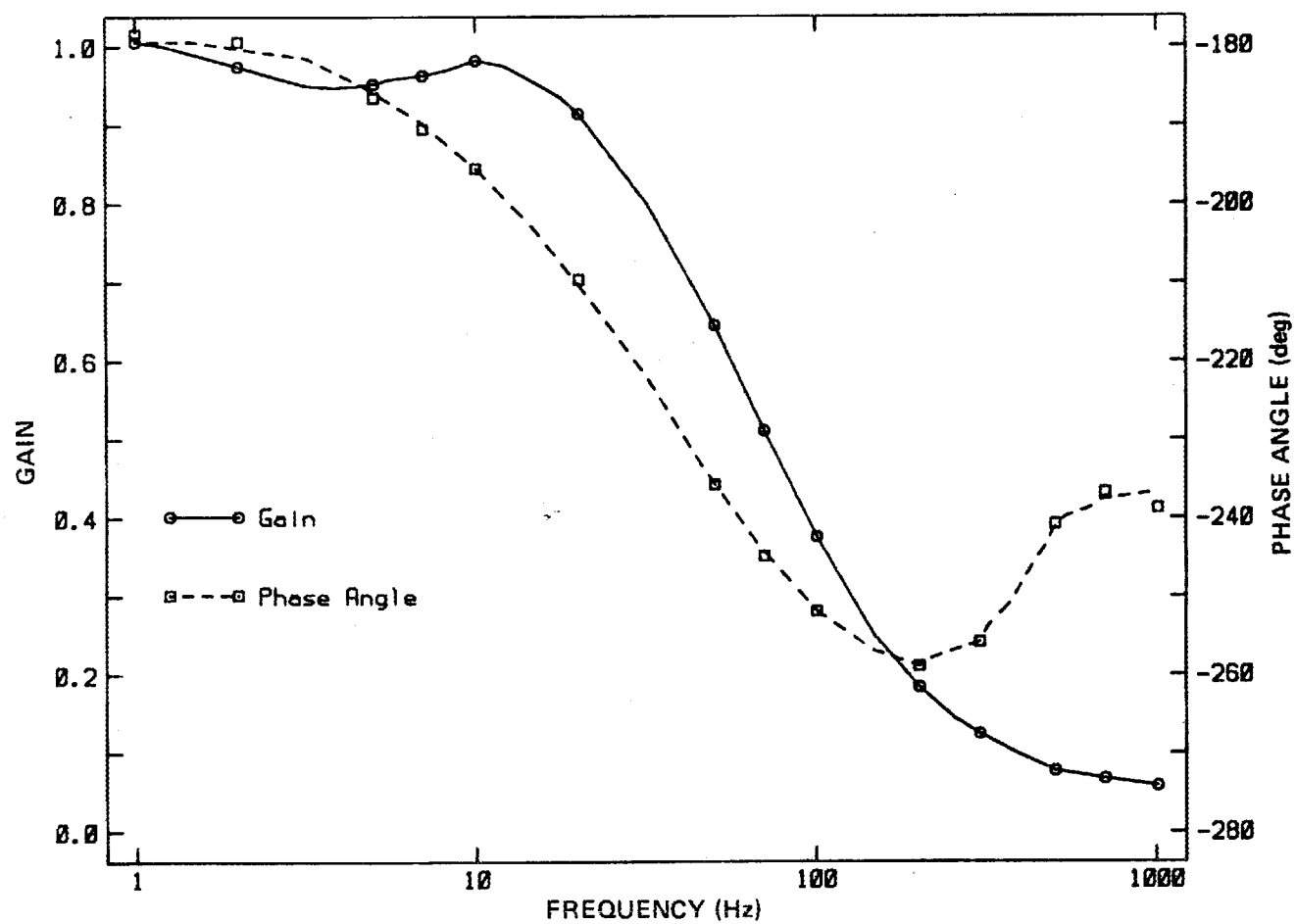


Fig. 3.5. Transfer function of the potentiostat electrochemical cell control system of the amperometric titrator: $E_{\text{Applied}} = 1.0 + 0.1 \sin(2\pi ft)$ V vs SCE.

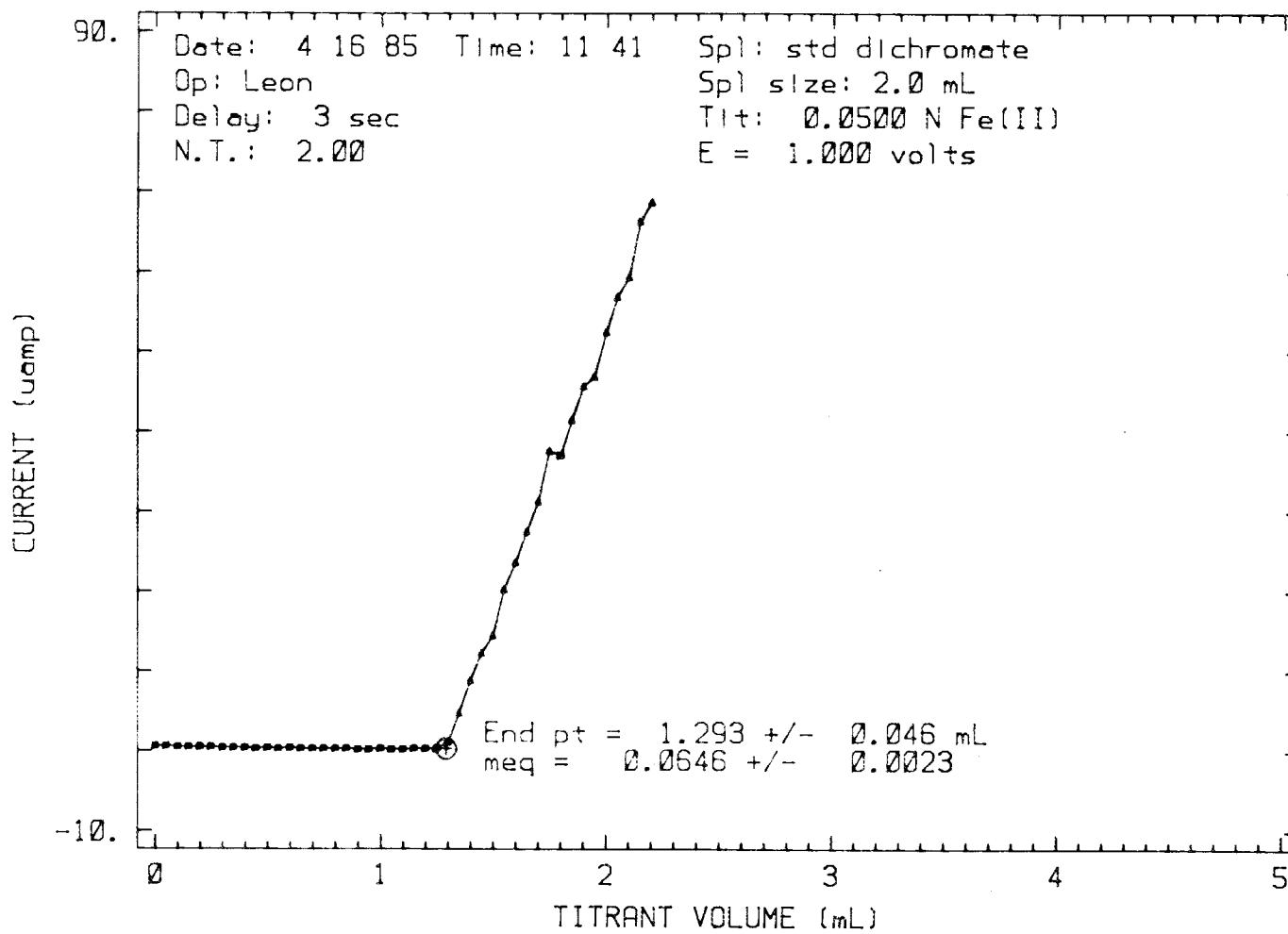


Fig. 3.6. Amperometric titration of $K_2Cr_2O_7$ with Fe(II).

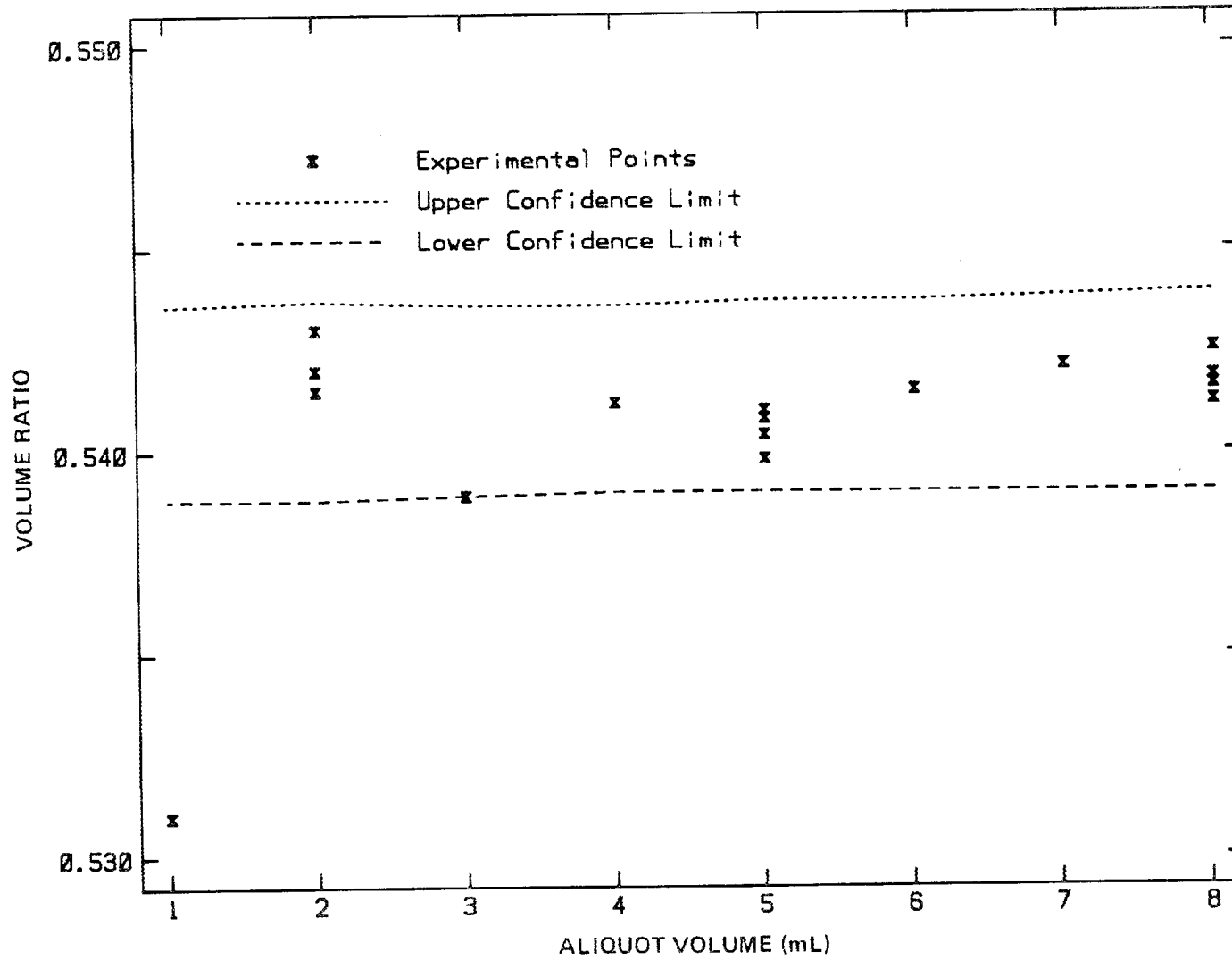


Fig. 3.7. Summary of the evaluation of the amperometric titration system.

Because of the method used to calculate the end point of the linear titrations, an estimate of the uncertainty of each individual end point value can be obtained. This uncertainty is obtained by propagating the calculated standard deviations of the slopes and intercepts of the line segments defining the pre-end point and post-end point regions of the titration curve into the uncertainty of their intersection. It was predicted from simulation studies that the mean of replicate titrations would show a significantly smaller uncertainty than the individual end points and that this uncertainty is related to the noise on the measured signal. These results were confirmed experimentally. Typical results for two different aliquots of $K_2Cr_2O_7$, are shown in Table 3.7. The uncertainty for the mean volume is the standard deviation of the mean for the number of replicates shown. This result suggests that the standard deviation of the mean of replicate titrations will underestimate the standard deviation of the final analytical result; error propagation procedures and the standard deviation of the individual values should be used to estimate the standard deviation of the final results.

Table 3.7. Uncertainty of individual end points compared to the precision of the mean end point volume

Sample volume (mL) ^a	End point (mL)	Mean volume (mL)
2.00	1.083 ± 0.007	1.084 ± 0.001
	1.084 ± 0.009	
	1.086 ± 0.009	
	1.084 ± 0.007	
8.00	4.340 ± 0.086	4.334 ± 0.004
	4.333 ± 0.014	
	4.330 ± 0.027	
	4.334 ± 0.008	

^amL of 4.181 mM $K_2Cr_2O_7$.

REFERENCES

1. J. J. Lingane, "Automatic Potentiometric Titrations," *Anal. Chem.* **20**, 285-292 (1948).
2. H. V. Malmstadt and E. R. Felt, "An Automatic Differential Potentiometric Titrator," *Anal. Chem.* **26**, 1348-1351 (1954).
3. M. T. Kelley, D. J. Fisher, and E. B. Wagner, "Automatic Recording Velocity-Servo Potentiometric Titrator," *Anal. Chem.* **32**, 61-66 (1960).
4. D. Jagner, "A Semi-Automatic Titrator for Precision Analysis," *Anal. Chim. Acta* **50**, 15-22 (1970).
5. J. J. Kankare, P. O. Kosonen, and P. O. Vihera, "Automatic Titrator for Digital Recording of Potentiometric Titration Curves," *Anal. Chem.* **46**, 1362-1364 (1974).
6. D. Betteridge et. al., "Application of Microprocessors to Chemical Analysis: Sequential Titration of Adipic and Boric Acid," *Analyst* **101**, 409-420 (1976).
7. N. Busch, P. Freyer, and H. Szameit, "Microprocessor Controlled Differential Titrator," *Anal. Chem.* **50**, 2166-2167 (1978).
8. R. Guevremont and B. Kratochvil, "Automatic Gravimetric Titration System," *Anal. Chem.* **50**, 1945-1948 (1978).
9. A. H. B. Wu and H. V. Malmstadt, "Versatile Microcomputer Controlled Titrator," *Anal. Chem.* **50**, 2090-2096 (1978).
10. C. R. Martin and H. Freiser, "Microcomputer Controlled Potentiometric Analysis System," *Anal. Chem.* **51**, 803-807 (1979).
11. R. E. Cover and L. Meites, "Automatic and Coulometric Titrations in Studies of Chemical Kinetics. I. Complex Formations," *J. Phys. Chem.* **67**, 1528-1533 (1963).
12. J. G. McCullough and L. Meites, "Titrimetric Applications of Multiparametric Curve Fitting: Locations of End Points in Amperometric, Conductometric, Spectrophotometric, and Similar Titrations," *Anal. Chem.* **47**, 1081-1084 (1975).
13. J. W. Frazer, W. Selig, and L. P. Rigdon, "Equivalence Point Determination for Automated Potentiometric Titrations with Ion-Selective Electrodes," *Anal. Chem.* **49**, 1250-1255 (1977).
14. M. Bos, "An Online Computer Method for the Potentiometric Titration of Mixtures of a Strong and Weak Acid," *Anal. Chim. Acta* **90**, 61-69 (1977).
15. T. W. Hunter, J. T. Sinnamon, and G. M. Hieftje, "Evaluation of Unique Directly Digital Computer-Controlled and Hardware-Controlled Automatic Titrators," *Anal. Chem.* **47**, 497-502 (1975).
16. T. F. Christiansen, J. E. Busch, and S. C. Krogh, "Successive Determinations of Calcium and Magnesium in Drinking Water by Complexometric, Potentiometric Digital Titration to Two Equivalence Points," *Anal. Chem.* **48**, 1051-1056 (1976).
17. D. J. Leggett, "Microcomputer Controlled Potentiometric Titration System for Equilibrium Studies," *Anal. Chem.* **50**, 718-722 (1978).

18. J. C. Smit and H. C. Smit, "Computer-Controlled Titrations: Part 1. Considerations Based on Systems Theory," *Anal. Chim. Acta* 143, 45-77 (1982).

19. D. E. Goeringer and L. N. Klatt, "Microcomputer Controlled Hot-Cell Pipetting System," *Anal. Chem.* 54, 1902-1904 (1982).

20. "Operation of Remote Titration System, ORNL Model Q-5895, for Potentiometric Titrations," Standard Laboratory Procedures, Process Methods, No. 1 003111, Analytical Chemistry Division, Oak Ridge National Laboratory, February 1985.

21. A. Savitzky and M. J. Golay, "Smoothing and Differentiation Data by Simplified Least Squares Procedures," *Anal. Chem.* 36, 1627-1639 (1964).

22. "Chemical, Mass Spectrometric, and Spectrochemical Analysis of Nuclear Grade Plutonium Dioxide Powders and Pellets," Annual Book of ASTM Standards, Vol 12.01, C 697-86, American Society for Testing and Materials, Philadelphia, PA, 1987.

INTERNAL DISTRIBUTION

- | | |
|--------------------|------------------------------------|
| 1. D. E. Benker | 23. E. H. Krieg, Jr. |
| 2. J. E. Bigelow | 24. S. A. Meacham |
| 3. D. A. Bostick | 25. D. R. Moser |
| 4. J. L. Botts | 26. R. E. Norman |
| 5-7. W. D. Burch | 27. F. L. Peishel |
| 8. J. A. Carter | 28. J. M. Ramsey |
| 9. J. Y. Chang | 29. J. H. Shaffer |
| 10. D. A. Costanzo | 30. W. D. Shults |
| 11. M. H. Ehinger | 31. B. B. Spencer |
| 12. M. J. Feldman | 32-33. J. G. Stradley |
| 13. W. S. Groenier | 34. K. U. Vandergriff |
| 14. D. W. Jared | 35-36. Laboratory Records |
| 15. R. T. Jubin | 37. Laboratory Records,
ORNL-RC |
| 16. R. K. Kibbe | 38-39. FRD Publications Office |
| 17. L. J. King | 40. ORNL Patent Section |
| 18-22. L. N. Klatt | |

EXTERNAL DISTRIBUTION

41. D. E. Bailey, Director, Division of Fuels and Reprocessing, Office of Facilities, Fuel Cycle, and Test Programs, NE-471, U.S. Department of Energy, Washington, DC 20545.
 42. F. P. Baranowski, 657 Fairfax Way, Williamsburg, VA 23185.
 43. M. J. Ohanian, Associate Dean for Research, College of Engineering, 300 Weil Hall, University of Florida, Gainesville, FL 32611.
 44. M. J. Rohr, Program Manager, Consolidated Fuel Reprocessing Program, Energy Programs Division, Energy Technology Branch, Oak Ridge Operations Office, U.S. Department of Energy, P.O. Box 2001, Oak Ridge, TN 37831.
 45. Office of Assistant Manager for Energy Research and Development, DOE-ORO, Oak Ridge, TN 37831.
- 46-117. Given distribution as shown in TIC-45900 under UC-526, Consolidated Fuel Reprocessing Category.

